Biomedical Signal Processing and Control 51 (2019) 171–180

Contents lists available at ScienceDirect

Biomedical Signal Processing and Control

journal homepage: www.elsevier.com/locate/bspc

Standard ECG lead I prospective estimation study from far-field bipolar leads on the left upper arm: A neural network approach☆

Pedro R. Vizcaya[a], Gilberto I. Perpiñan[b,1], David J. McEneaney[c], Omar J. Escalona[d,*]

[a] The School of Engineering, Pontificia Universidad Javeriana, Bogotá, 110231, Colombia
[b] The Faculty of Electronic and Biomedical Engineering, Universidad Antonio Nariño, Cartagena, Colombia
[c] The Cardiovascular Research Unit, Craigavon Area Hospital, Portadown, BT63 5QQ, UK
[d] The Engineering Research Institute, Ulster University, Newtownabbey, BT37 0QB, UK

ARTICLE INFO

Article history:
Received 24 July 2018
Received in revised form
31 December 2018
Accepted 7 January 2019

Keywords:
Electrocardiography
Biomedical monitoring
Wearable sensors
Biological information theory
Mutual information
Artificial neural network

ABSTRACT

In this study, the feasibility of interpreting heart rhythms from far-field bipolar ECG arm-band lead recordings on the left-upper-arm (LUA), is evaluated in a clinical multichannel arm-ECG mapping database (N = 153 subjects) for the prospective development of long-term heart rhythm monitoring from comfortable arm wearable devices. A preliminary multivariable linear regression analysis on ECG chest Lead I from 10 selected far-field bipolar leads along the left arm, indicated that 3 of them in the LUA were relevant and worth evaluating in more detail from a heart rhythm information perspective.

To derive a good and effective estimation process, a time series non-linear regression point estimator, using an artificial neural network with 2 lags was investigated, showing a correlation coefficient of up to 0.969 for a single subject. Then, a vector approach was adopted for the whole LUA database, aiming to develop a subject independent estimation process of the P-QRS-T waveform interval and its heart rhythm attributes in the standard chest Lead I. In the same study, the first 96 coefficients, of the Discrete Cosine Transform on the P-QRS-T interval were used as a means for reducing the dimensionality of the input space, with a loss of just 0.1% in power, and reducing the dimensionality to just 5% of the original size. The trained ANN for ECG Lead I estimation from one upper arm Lead-1 showed a correlation coefficient above 80% on a beat-to-beat basis, an improvement on all but 1.34% of the beats estimated for a typical train/test partition of the LUA database. The non-triviality of the results was tested with random and intentional true negatives. Information theory analytics revealed that there is an estimated information of 1.6 bits/beat between LUA armband bipolar leads and the standard Lead I.

1. Introduction

Cardiovascular risk and diseases are a major determinant of global health [1]. Furthermore, patients with palpitations or loss of consciousness (syncope) account for a large proportion of attendances at hospital outpatients and emergency rooms [2]. In particular, cardiovascular disease (CVD), is the most common underlying cause of death in the world, accounting for an estimated 31.5% of all global deaths [3]. The electrocardiogram (ECG) has been the standard clinical tool for investigating the electrical conduction in the heart, and for monitoring its ventricular stability, by means of arrhythmic episode detection and by heart rhythm characterisation in standard ECG recordings. At risk patients present transient abnormal heart rhythms (arrhythmias) which are important in the diagnosis of heart disease and have prognostic significance [1]. As there are many different cardiac arrhythmias, their accurate detection and recording is an important clinical need and thus, continuous monitoring of the patients' heart rhythm is required for periods lasting from several days, up to a number of years, in order to enable the detection of transient arrhythmias at an early stage of heart disease, which would improve the effectiveness of appropriate treatment, reducing disease burden, disability and death. However, transient arrhythmias lasting only a few seconds are clinically difficult to detect [4].

☆ This work was supported by funds from the European Union (EU): Horizon 2020 Marie Skłodowska-Curie Actions (MSCA) RISE Programme (WASTCArD Project, Grant #645759). Professor O. Escalona's work was supported by funds (CACR Project) equally from: the Ulster Garden Villages and the McGrath Trust, both based in the UK.

* Corresponding author.
E-mail addresses: pvizcaya@javeriana.edu.co (P.R. Vizcaya), gilberto.perpinan@uan.edu.co (G.I. Perpiñan), david.mceneaney@southerntrust.hscni.net (D.J. McEneaney), oj.escalona@ulster.ac.uk (O.J. Escalona).

[1] Formerly was with the Electronics and Circuits Department, Universidad Simón Bolívar, Caracas, 89000, Venezuela; during the early part of the research work.

https://doi.org/10.1016/j.bspc.2019.01.020

Continuous monitoring of human physiological parameters is becoming increasingly important. In general there are two approaches to long-term cardiac rhythm monitoring. a) Event recorders are non-invasive recording devices with sensing electrodes attached on the patient's body surface, usually on the chest wall; nevertheless, they are inconvenient (uncomfortable) for the patient and only suitable for short term recordings. b) Implantable loop recorders are implanted subcutaneously on the chest wall; however, while they are capable of monitoring heart rhythm during very long periods, there are considerable costs associated with the device itself and hospitalisation costs; besides the risks of surgery including infection [5]. Currently available cardiac monitoring arm/wrist bands do provide support in monitoring the heart rate; however, these cannot continuously capture ECG heart rhythm attributes provided within the heart beat P-QRS-T waveform interval. With CVD and lethal heart arrhythmias continuing to have a high mortality rate, it is important to provide patient compliant solutions for non-invasively monitoring the heart rhythm information in the P-QRS-T interval of the ECG from a long-term wearable device placed on comfortable positions of the body, such as along a single arm (armband) [6], or ideally on the wrist. The challenges of this approach lie in the difficulty of detecting an adequate bipolar ECG signal due to the low amplitude and excessive muscle artefact in these far-field ECG locations [7].

At our Engineering Research Institute, we have developed various low-amplitude electrocardiographic signal recovery techniques in the past few years [8–10]. This platform of knowledge and expertise has been combined with more recent ECG denoising techniques, such as empirical mode decomposition (EMD) and enhanced EMD (EEMD), to address the aforementioned far-field arm-ECG recovery problem [11,12]. Of particular interest in this study is the information theory perspective of estimation capacity for a selected standard chest ECG lead signal, such as ECG Lead-I from a selection of far-field bipolar leads on the left-arm.

Currently, there are many clinical applications for estimating and reconstructing signals, for example, in estimating the respiratory rate [13] and blood pressure using ECG characteristics. Also, for estimating the precordial ECG leads from the standard limb leads (Lead I, Lead II and Lead III) [14]. Other efforts have been invested on the far-field estimation of the 12-lead ECG from intracardiac electrograms, using for this purpose nonlinear estimation methods based on artificial neural networks (ANN) [15].

In previous studies [16,17], it has been indicated that certain far-field bipolar ECG recordings along the left-arm, present sufficient information of standard electrocardiographic features to be of diagnostic clinical value. In those reports, far-field bipolar ECG leads on the left upper-arm, provided a stronger signal with gelled BIS^{TM} sensor system than dry AgCI electrodes. Therefore, it would be valuable to objectively assess the information capacity metrics [18] on the left upper-arm bipolar leads, enabling reliable estimate of the standard ECG chest Lead I.

The purpose of the present study is to establish whether or not and to what extent and conditions, the feasibility of reconstructing the standard ECG Lead I from the ECG information extracted from left-arm bipolar ECG lead recordings after noise reduction. To such extent, the ECG signal may be generally categorised as a quasi-periodic cyclostationary random process [19]. Basic multivariable linear regression models [20], as well as the ensemble average, may be used to estimate the significance of different ECG lead arrays. Principal component analysis (Eigen vector and values) is also useful for this approach [21]. Then, the dimensionality of ECG P-QRS-T waveform complex (given the quasi-periodic hypothesis), can be substantially reduced with the discrete cosine transform (DCT). With a reduced dimensionality of the ECG complex ensemble, it is then possible to generate a time series non-linear estimator using artificial neural networks.

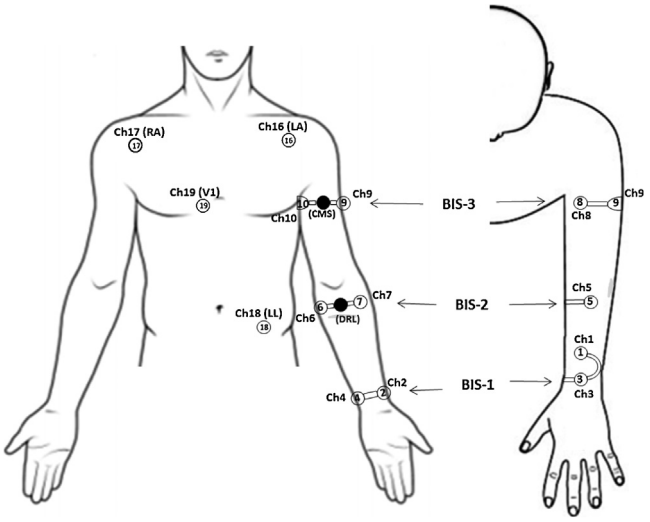

Fig. 1. Location of left-arm recorded channels sensors.

In the recent paper addressing the problem of reconstructing precordial leads from limb leads [14], based on a state variable estimator that models the time relationship between leads, they report final correlation coefficients as high as 0.98 for estimation analysis on a single subject, showing again that ECG is a quasi-stationary process. In our study, the estimation is not restricted to a subject. Our objective is to derive an estimation process which would be **subject independent**. Hence we utilise every full P-QRS-T interval as a vector for every heartbeat, and a sequence of this vectors as the time sequence.

Information theory has been used for 70 years as a solid framework for data analysis [18]. Surprisingly, its use in signal processing is relatively recent and has been limited. Mutual information is an objective measure of the information content of a variable relative to another variable; it is measured in bits. However, the correlation coefficient is still the most widely used parameter because of its mathematical treatability [20]. Our study includes a basic analysis of performance of the estimator using both approaches.

This paper is organized as follows: the Methods section presents the characteristics of the database of patients' electrograms and the flowchart of the main processing steps and algorithms for pre-filtering, P-QRS-T waveform detection and selection, and the ANN based estimation process. The following section presents the results of feature extraction, training and testing of and ANN, and the performance evaluation of the estimation process. The last section, presents a discussion and the conclusions of the work.

2. Methods

2.1. Arm-ECG mapping

In this study, three leads derived from the upper arm are tested for the estimation of Lead I. Fig. 1. illustrates the location of sensors used in this study. Table 1 describes the location of the leads used for the estimation of Lead I, the conventional chest lead.

Lead 1 is transversal, bipolar, Lead 2 is front-back, and Lead 3 axial, upper arm-forearm.

2.2. Clinical database

This study is carried out on a population of 153 subjects (99 women and 54 men), aged between 19 and 82 years, whose exclu-

Table 1
Channel sensors pair associated to the selected bipolar leads.

Name	Sensor	Description
Lead I	Ch16-Ch17	Conventional chest lead.
Lead-1	Ch9-Ch10	Transversal, bipolar upper arm, lateral.
Lead-2	Ch8-CMS	Transversal, upper arm, front-back 90°
Lead-3	Ch7-Ch10	Axial; upper arm – forearm.

Table 2
Baseline characteristic of the 153 subjects (99 women and 54 men) under study. SD stands for standard deviation, IQR for interquartile range.

Characteristics	Mean	SD	Median	IQR
Age (year)	42.9	17.4	45	26.3
Height (m)	1.5	0.5	1.7	0.1
Weight (Kg)	70.3	29.5	76	22
BMI	24.3	10.6	26	7
Pulse (bpm)	73.5	14.1	73	17.5
Systolic pressure (mm Hg)	126.8	22.2	125	28.3
Diastolic pressure (mm Hg)	70.7	12.8	70	16.3

sion criterion is the presence of atrial fibrillation. The database was collected in the Cardiovascular Research Unit at Craigavon Area Hospital, located in Portadown (Northern Ireland). All subjects agreed to the study by signing an informed consent. Ethical approval was obtained from HSC REC B (Health and Social Care, Research Ethical Committee, reference: 16/NI/0158), and IRAS (Integrated Research Application System, registered project ID: 203125, dated: 21/September/2016).

Table 2 summarises the characteristics of the study population.

Recordings were carried out on different days using the same room environment and recording equipment. The recording duration of the multichannel ECG (14 unipolar channels with the reference electrode [CMS] positioned on the upper arm) for each subject was 500 s, at a sample rate of 2048 Hz, and a nominal resolution of 24 bit. All subjects were recorded in their resting position. To gather a clinical database of left-arm ECGs under ethical approval, a sensor system with known high performance on the skin–electrode interface impedance and good potential stability, the BIS-Quatro™ (four-electrode) sensor (Covidien, Mansfield, MA, USA) are used.

2.3. Estimation process

From our preliminary analysis of the arm leads on 12 subjects, it was clear that some of the there was signal information loss of ECG Lead I features as a consequence of signal attenuation along distance and muscle artefact arising from the arm. Our preliminary analysis also showed that this was subject dependent. Also, a multivariable linear regression analysis on Lead I from 10 leads taken from the left arm showed that up to 3 of them were relevant. The R-squared statistics (relation between error variance and signal variance) showed a moderated average value of 0.443 between the estimated and the real Lead I. In order to obtain a better estimation, a time series non-linear regression point estimator using an artificial neural network with 2 lags was tested; which means that the current beat and the two previous ones were used, showing a correlation coefficient of up to 0.969 for a single subject, very much in agreement with [14]. This shows that the ECG signal may be considered as a quasi cyclostationary random process. The random part, when the ECG is taken in rest, supine position, is the latency of the P-QRS-T waveform; this explains why the correlation coefficient between waveforms of the same subject is very high [14]. Thus, we concluded that a larger database was necessary in order to be able to develop a waveform approach for a **subject independent** estimation of Lead I.

In our pilot study, the Discrete Cosine Transform (DCT) on the P-QRS-T waveform was tested as a means for reducing the dimensionality of the input space. A typical P-QRS-T waveform interval is close to 2000 samples long. The objective was to select a sufficient number of first 96 coefficients (discarding the DC component), representing a low percentage of the original dimensionality, but nonetheless retaining a high percentage (> 99.5%) of the power of the signal.

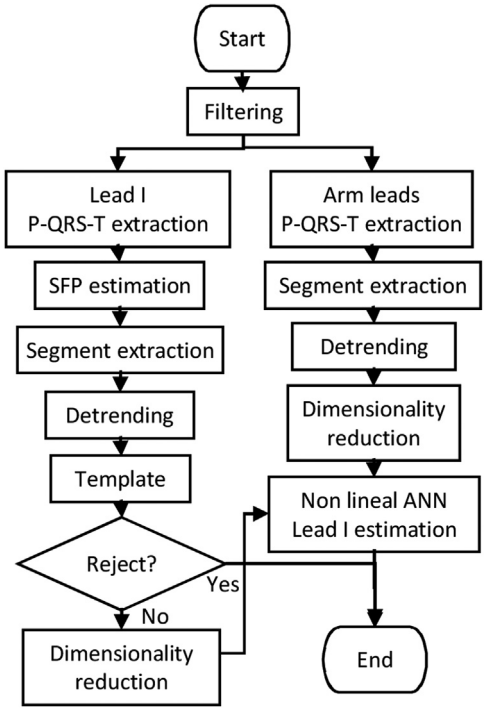

Fig. 2. Overall study methods flowchart for the implemented estimation process of Lead I.

For the present study, the following steps on the ECG Lead I and its arm leads ANN estimation are performed, as summarized in the flowchart presented in Fig. 2:

Step1. Filtering. Linear filters are used to attenuate power line interference, reduce out-of-band noise, and limit the signal bandwidth. A second order high pass Butterworth filter at 0.2 Hz is used to limit DC wandering due to respiratory artefact. A second order low pass Butterworth filter at 40 Hz is used to limit the bandwidth of the signal and attenuate out of band noise and the power line interference. A Q = 20 notch filter designed at 50 Hz is used to cancel the power line influence. These filters were applied offline backward and forward to reduce group delay differences as a function of the frequency. The cut frequencies were chosen for ECG monitoring purposes.

Step 2. P-QRS-T segment extraction. Chest Lead I was used to obtain the single fiducial point (SFP) of ventricular depolarisation events. The location of the SFP referring to ventricular activity is obtained by filtering the signal with a band pass filter with cut-off frequencies at 3 and 30 Hz, then zero-level crossing is located in the RS interval. Based on the maximum value R_{max} within a time window starting at 20 s and spanning 50 s, the algorithm then proceeds to search for signal values above the threshold 60% of R_{max} followed by zero-level crossing; if the number of samples of the signal in this RS interval is contained within a valid time duration criteria of minimum time, RDTMIN = 15 samples time, and maximum, RDTMAX = 50 samples, the QRS complex is validated and its corresponding SFP is recorded. The extracted SFP time-series was then used to ensemble a 700 ms signal window, centred around every time element of the SFP time-series (from 400 ms before the SFP and 300 ms after the SFP), for every arm-ECG bipolar lead signal. The SFP is used for segmenting three arm-ECG bipolar leads,

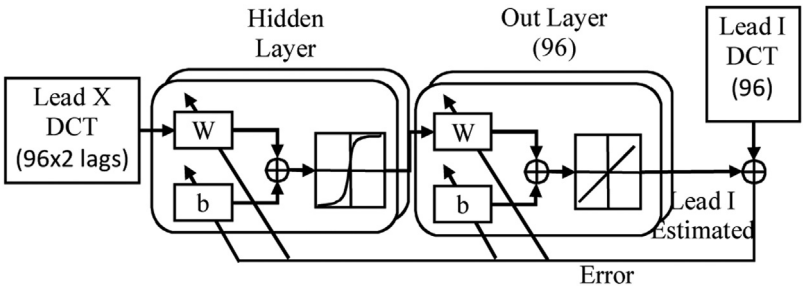

Fig. 3. Artificial neural network for estimation of Lead I. The size-5 hidden network, having the Lead X-DCT (X = 1,2 or 3) vector as its input, is adapted with the error to minimize the difference between the estimated Lead I DCT vector, built with the output layer which is also updated through error feedback (backward error propagation training mode).

consecutively aligned ventricular depolarization events; around 70 heartbeats or more were included in each subject case for further processing. Detrending was applied to every segment to further reduce wandering. 35 out 153 subjects with excessively noisy or abnormal beats (less than 50% of similarity among beats with a template of the first 40 beats as measured with its correlation coefficient) were excluded. A total of 8260 beats, 70 beats for each 118 subjects were retained.

DCT dimensionality reduction. As pointed out before, the DCT is used to reduce the dimensionality of the signal space. The DCT has properties related to Markov processes: its correlation matrix is similar to the correlation matrix of a first order Markov process, which makes it as close as possible to the optimal transform for compression (the Karhunen-Loeve transform) for processes for which first order dominates the behaviour, with the advantage of being fixed and independent of the actual autocorrelation. In contemporary practise DCT is a standard procedure for signal compression for 1-D and 2-D processes. The Discrete Cosine Transform (DCT) on the P-QRS-T waveform was calculated for reducing the dimensionality of the input space.

Step 3. Arm leads (1–3) are filtered as described in Step 1. The extraction of the P-QRS-T segment uses the information found from its corresponding Lead I segment, in Step 2. Detrending is used to supress the wandering reminding after the application of the 0.4 Hz high pass filter. Dimensionality reduction follows the same procedure described in Step 2 for Lead I.

Step 4. In this step, a time series non-linear NN vector estimation of Lead I is implemented. For this, a non-linear artificial neural network (ANN) is trained to estimate the corresponding Lead I P-QRS-T DCT based on each of the three LUA leads considered. In the considered bipolar arm leads 1–3 (see Table 1), the DCT is normalized (both DC and standard deviation). In the preliminary study it was found that a size 5 hidden network with 2 input delays was necessary to obtain the best match between input and output, as an increase in the size of the hidden network or the number of delays did not improve performance significantly. The ANN architecture is shown in Fig. 3.

The training algorithm used for the feed-forward back-propagation time-series ANN is the Levenberg-Marquardt method, and the optimization criteria is to minimize the mean squared error between the reference Lead I DCT, and the estimated one. So, the correlation coefficient between these two vectors, ρ, is a good indicator of its performance [20], defined as shown in Eq. (1).

Note that the correlation coefficient evaluated on the DCT is equivalent to the correlation coefficient evaluated on the original time space, since the DCT is a linear transformation (and so it does not change the shape of the space) since the Parseval's relationship between the two spaces applies.

$$\hat{\rho} = \frac{\sum_{i=1}^{96} \left(AL_i - \hat{\mu}_{AL}\right)\left(LeadI_i - \hat{\mu}_{LeadI}\right)_i}{\hat{\sigma}_{AL}\hat{\sigma}_{LeadI}}$$

with

$$\hat{\mu}_{AL} = \frac{1}{96}\sum_{i=1}^{96} AL_i,\ \hat{\mu}_{LeadI} = \frac{1}{96}\sum_{i=1}^{96} LeadI_i$$

and

$$\hat{\sigma}_{AL} = \sqrt{\frac{1}{95}\sum_{i=1}^{96}\left(AL_i - \hat{\mu}_{AL}\right)^2},$$

$$\hat{\sigma}_{LeadI} = \sqrt{\frac{1}{95}\sum_{i=1}^{96}\left(LeadI_i - \hat{\mu}_{LeadI}\right)^2}, \quad (1)$$

where

AL : Arm Lead DCT,

LeadI : Lead I DCT.

Moreover, the following transformation of the correlation coefficient renders a Gaussian random variable [20] (p. 434):

$$X = \frac{1}{2}\ln\left(\frac{1+R}{1-R}\right)$$

$$\mu_X = \frac{1}{2}\ln\left(\frac{1+\rho}{1-\rho}\right)$$

$$\sigma_X^2 = \frac{1}{n-3} \quad (2)$$

$$z = \frac{\sqrt{n-3}}{2}\ln\left(\frac{1+r}{1-r}\frac{1-\rho_0}{1+\rho_0}\right)$$

In Eq. (2), R is any estimator of the correlation coefficient seen as a random variable, X is its transform which has Gaussian distribution, so after normalizing it, by subtraction of its mean and division by its standard deviation, a normal Gaussian Z distribution is obtained for hypothesis testing using a z or t-student distribution.

The ANN is initially trained with a selection of heartbeats taken from up to 118 subjects. A subject is included in the selection if his/her ECG record satisfies the acceptance fidelity criteria. The criteria applied is as follows: first a P-QRS-T template pattern based on Lead I is built by averaging the first 40 beats; then every beat is tested against this template using their correlation coefficient as an indicator. If the beat satisfies a given threshold for this correlation, then it is accepted. If the whole record satisfies a given number of accepted beats (70 for this experiment), then the subject is accepted, otherwise is rejected for training.

This training set is divided randomly into three subsets: 70% for training properly, 15% for validation (during training, this set is used as a way to know when to stop the training procedure), and 15% for testing. This procedure assures that the ANN is not over trained and that it will generalize, as far as the database used for training is statistically representative of the whole population. The distribution of the correlation coefficient between the original arm lead (1, 2 or 3) and the original Lead I, is compared to the correlation coefficient between the estimated Lead I and the actual Lead I to evaluate the performance of this process.

The ANN, trained as described above, is then tested against the best 70 beats (relative to its template according to the correlation test) of the subjects not included in the training process. Its performance is evaluated using the same procedure as above.

2.4. Performance evaluation

The standard approach for evaluating the performance of the estimation process is through the analysis of the **correlation coefficient** between the estimated Lead I and the original Lead I. As a starting point for comparison, the correlation coefficient between the original Lead-1 and the original Lead I is evaluated as a baseline. And finally, to test whether the ANN is using the current information on Lead-1 or it has just learned the mean relationship between Lead 1 and Lead I, the trained ANN is tested with random Lead-1 waveforms taken from different subjects. This comparison tells us whether ANN is actually using the information of the current Lead 1 or it is just using a memorized mean waveform.

An alternative way to evaluate the performance of the estimator is using **information theory** concepts [18]. Evaluation based on correlation, as before, hides the real information content of a signal, as well as of the estimator. The first concept is to estimate the amount of information contained in the signal (DCT), which is called entropy. In order to estimate its entropy, the signal DCTs are classified in a finite number of prototype DCTs; the process is called vector quantization (VQ) or k-means. The parameter k is the number of classes; it has to be selected based on an expected amount of information or a given mean square error tolerance of the VQ process. The signal DCT is then encoded with the VQ as an index out of k.

Once both signal DCTs (the original and the estimation) are encoded with the VQ entropy is estimated from the probability distribution function of their indices. The entropy is defined as [18]:

$$H(VQ_{DCT}) = -\sum_{i=0}^{k-1} p_i \log_2 p_i \text{[bits]} \tag{3}$$

where p_i is the probability of index i.

Then, the common information between the estimated DCT and the original DCT, which is called the mutual information, is estimated as follows:

$$I\left(VQ_{DCT_{LeadI}}; VQ_{DCT_{EstLeadI}}\right) = H\left(VQ_{DCT_{LeadI}}\right) + H\left(VQ_{DCT_{EstLeadI}}\right) - H\left(VQ_{DCT_{LeadI}}, VQ_{DCT_{EstLeadI}}\right)$$

where

$$H\left(VQ_{DCT_{LeadI}}, VQ_{DCT_{EstLeadI}}\right) = -\sum_{i=1}^{k}\sum_{j}^{k} p_{ij} \log_2 p_{ij} \tag{4}$$

is the joint entropy between Lead I and its estimation.

The concept of mutual information and its relationship with the joint entropy and marginal entropies, used in Eq. (4), is illustrated with a Venn Diagram, as shown in Fig. 4. It shows the mutual information between two random variables is the common information, and it shows the relationship with the joint entropy used in Eq. (4):

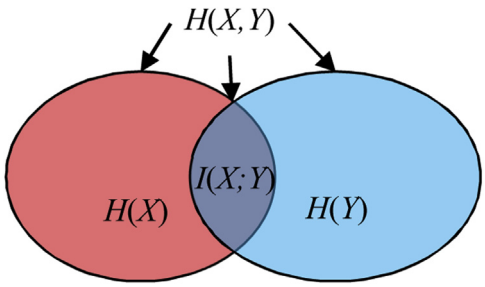

Fig. 4. Venn diagram showing graphically the relationship between marginal entropies, joint entropy and mutual information, as expressed in Eq. (5).

$$H(X, Y) = H(X) + H(Y) - I(X, Y) \tag{5}$$

3. Results

3.1. Heart beats inclusion process

Fig. 5 shows 70 heart beats (around 1 min) acquired transversely, on the left arm Lead-1 (Fig. 5a) and on chest Lead I (Fig. 5b). These P-QRS-T waveform intervals have been previously filtered and aligned, using the single fiducial point technique [9], and normalized (zero dc and unit variance). These beats have been chosen with 85% of similarity with an ensemble template built from the first 40 beats.

3.2. DCT transform

The first 96 coefficients of the DCT were chosen (excluding the zero dc component).

Fig. 6 illustrates the DCT sequence for the upper-arm Lead-1 (Fig. 6a) and for Lead I (Fig. 6b).

Notice that the ensemble of Lead I coefficients has smaller variance than the Lead-1 ensemble. The average correlation between Lead I waveforms for subject #1 is 0.96, while the average correlation for Lead 1 waveforms is 0.65.

Regarding dimensionality reduction performance, the analysis results revealed that the first 96 coefficients (discarding the DC component), just 5% of the original dimensionality, were sufficient to retain about 99.9% of the power of the signal.

3.3. Performance of the estimation process

Table 3 shows the mean (and standard deviation, sd) of the correlation values (ρ) when ANN is trained with different exclusion criteria among beats similarity: 93% means that only subjects with 70 beats with at least 93% of similarity among them were accepted. Training correlation values are better when similarity among beats increased and a few subjects are included, contrary with testing ones, correlation values are lower if ANN has been trained with low beats similarity percentage and many subjects from the database.

Fig. 7 compares the distributions (normalized histograms) for ρ train and ρ test for the two extreme cases considered in Table 3.

Table 3 and Fig. 7 show that as the fidelity criteria for testing is reduced, the testing distribution becomes closer, so it shows that it generalizes better. Comparison of the correlation coefficients between Lead-1 and Lead I for 85% correlation and the baseline are displayed in Figs. 8 and 9.

Fig. 8 shows the probability distributions of the transformed correlation coefficients for both the baseline and the estimator. They are clearly separated but overlapped.

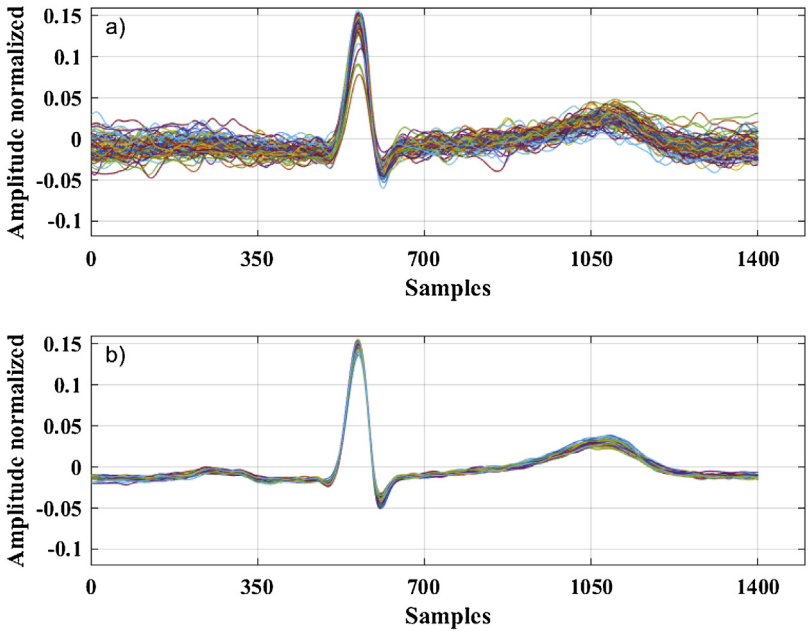

Fig. 5. 70 aligned beats from the subject Case #1 of the database; on the top (a), it shows left arm Lead-1 beats, and on the bottom (b) the chest Lead I P-QRS-T beat waveforms.

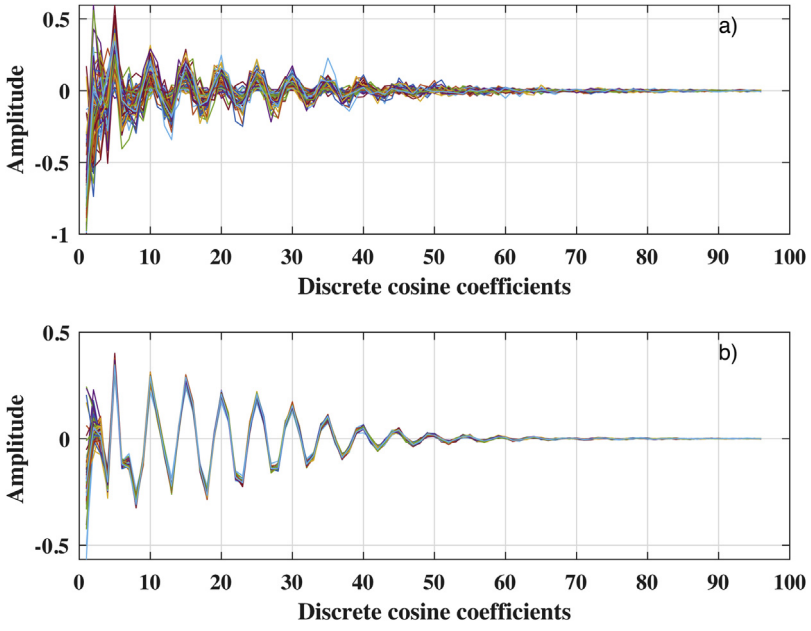

Fig. 6. Discrete cosine transform coefficients from several beats for subject #1. Top figure (a) shows left arm (Lead 1) and, bottom figure (b) shows chest Lead I. Beats from left arm are used as inputs in artificial neural network (ANN) and beats from chest lead as target inputs in the ANN.

Table 3
Training and test results of the ANN based on the left upper-arm Lead-1 only.

Values are mean (sd).				
	Correlation acceptance criteria			
	93%	90%	88%	85%
Number of subjects training/testing	37/57	51/55	59/37	68/30
ρ train mean (sd)	0.956 (0.054)	0.945 (0.065)	0.937 (0.072)	0.938 (0.06)
ρ test mean (sd)	0.801 (0.188)	0.824 (0.179)	0.825 (0.186)	0.807 (0.154)

sd: standard deviation.

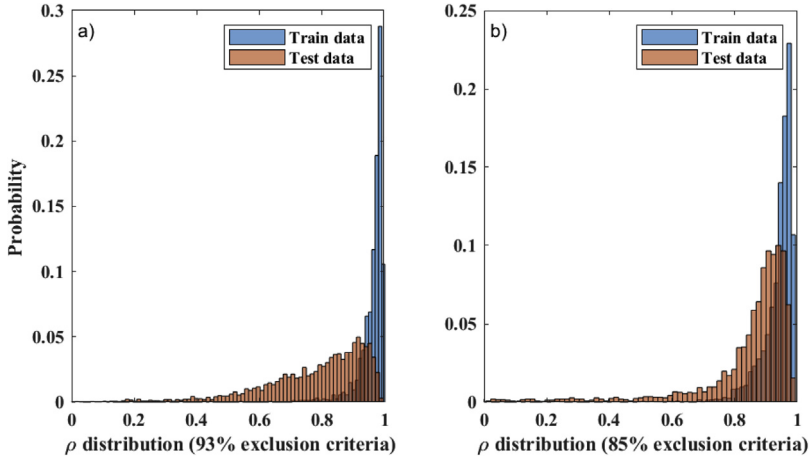

Fig. 7. Probability distribution of the correlation coefficients between estimated Lead-I and original Lead-I for the steps of training and testing of the ANN. On (a), left, for Correlation Criterion 93% and on (b), right, for 85%.

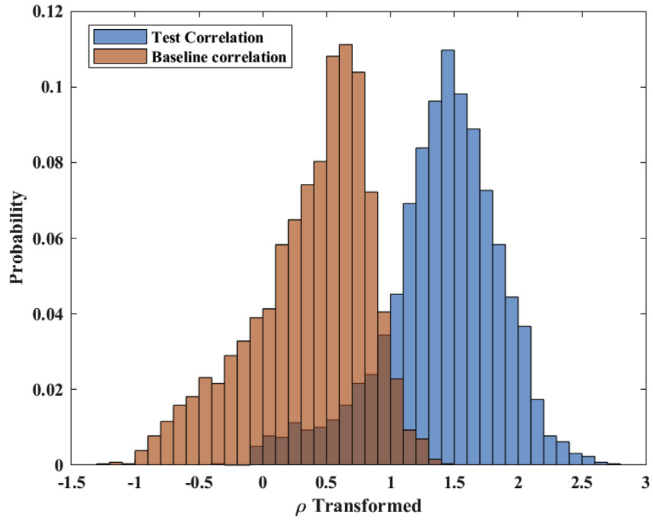

Fig. 8. Distribution of the baseline correlation (Lead-1 vs. Lead I) and estimated correlation (Lead-I estimated vs. Lead I).

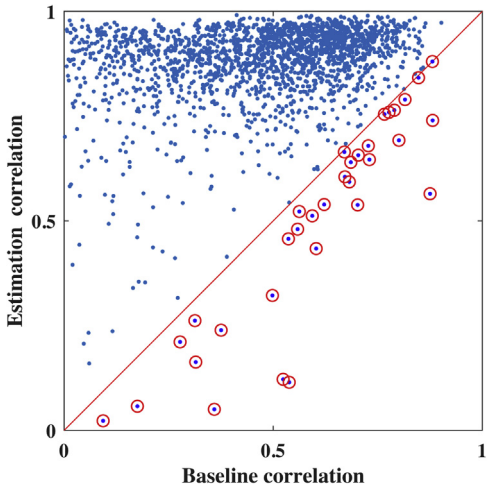

Fig. 9. Plot of baseline correlation and estimated correlation beats. Only 1.35% (red circles) of the baseline correlation did not improved after ANN process.

On the other hand, Fig. 9 shows the point spread of these correlation coefficients. Most of the beats improved their correlation after estimation (points above line). Only 35 out of 2588 beats did not improve (less than 1.4%).

Table 4
Training and testing results of ρ correlation performance of the ANN for chest Lead I estimation. Values are mean standard deviation (sd).

Correlation Criteria	Subjects train/test	Lead 2 ρ mean (sd)	Lead 3 ρ mean (sd)
95	15/74	0.694 (0.325)	0.554 (0.397)
93	15/74	0.741 (0.244)	0.650 (0.271)
90	38/55	0.771 (0.216)	0.725 (0.256)
88	51/42	0.710 (0. 299)	0.765 (0. 242)
85	59/37	0.793 (0.217)	0.813 (0.171)

Table 5
Summary of basic statistics of the ANN estimator using different leads.

	Lead 1 Mean (sd)	Lead 2 Mean (sd)	Lead 3 Mean (sd)
Baseline	0.371 (0.459)	0.181 (0.389)	0.199 (0.392)
Estimated Lead I	1.400 (0.459)	1.260 (0.570)	1.283 (0.529)

sd: standard deviation.

Lead I was also estimated using two more left arm lead (Lead-2 and Lead-3). Fig. 10 shows, 70 beats aligned for subject #1 from Lead-2 (Fig. 10a, top) and Lead-3 (Fig. 10b, mid.) compared with respective Lead I beats (Fig. 10c, bottom).

Table 4 summarizes the results on ρ for training and testing correlation performance with the ANN Lead I estimation, for left arm Lead-2 and Lead-3. Lead-3 results, using 85% of similarity, shows the best performance compared to estimation using Lead-2.

Table 5 summarizes statistics that allow us to compare the performance on estimation of the three leads considered. It turns out that Lead-1 (Table 3) offers the best estimation performance and capacity to reconstruct Lead I.

Fig. 11 presents a comparison plot of original and estimated heart beat in contrasting cases: Fig. 11a (top), a good case with a high correlation (0.99), and a bad case with low correlation of only 0.13 (Fig. 11b, bottom).

A basic null hypothesis test of this method was run using a random signal as input to the ANN. Fig. 12 shows the probability distribution of the correlation coefficient of the estimation with Gaussian noise: its mean is closer to 0 and its overlap with the distribution with the estimation based on Lead I is small. The mean of correlation transformed (mean (sd)) using as inputs Gaussian noise, 0.175 (0.33), is significantly different than the mean using as inputs Lead-1, 1.40 (0.45). Another test based on random selection of the Lead-1 DCT (instead of the corresponding to the Lead I), also reveals good performance, as presented in Fig. 13.

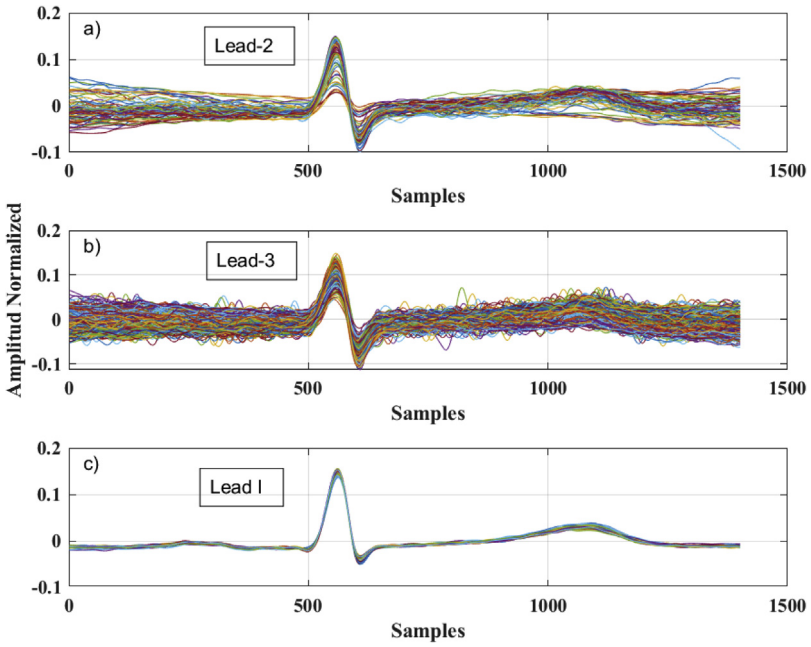

Fig. 10. 70 aligned beats from the same subject #1; on the top, it shows upper-arm Lead-2 (a), in the middle, Lead-3 (b) and in bottom, the chest Lead I (c).

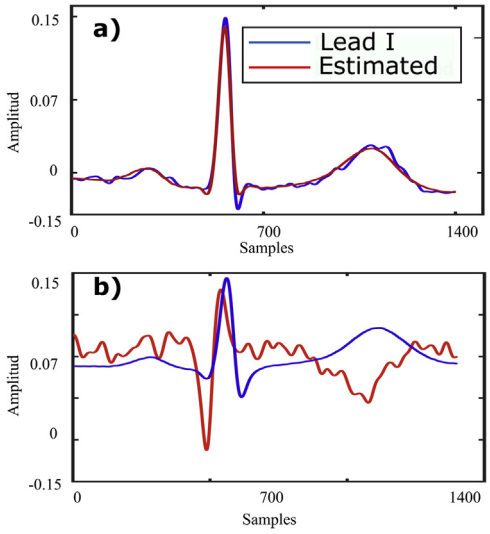

Fig. 11. Comparison of original and estimated heart beat (P-QRS-T waveform) for a well behaved case, top graph (a), with a high 0.99 correlation, and a bad case, bottom graph (b), with a poor correlation of 0.13.

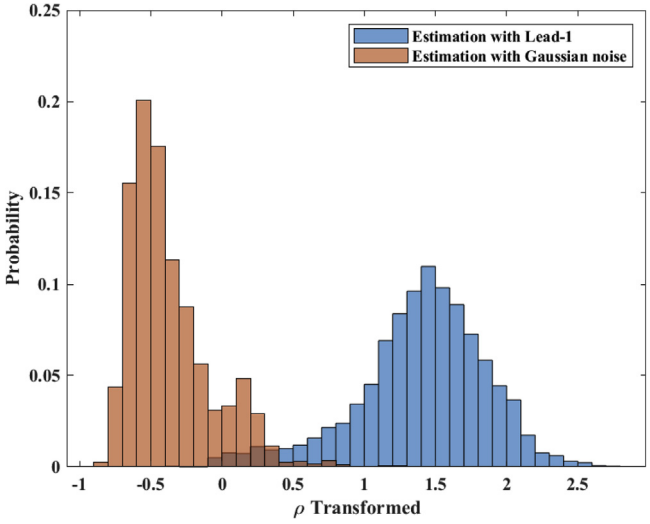

Fig. 12. Histograms of transformed correlation among Lead I and its estimation, when inputs to the ANN are Gaussian noise (brown) and Lead-1 (blue) correlation.

This figure shows the transformed correlation coefficient distributions between the random Lead-1 and Lead I, and the true Lead-1 and Lead I. The point spread shows more clearly their joint distribution, as presented in Fig. 14.

For the performance evaluation based on information theory concepts, the test database for 88% rejection criterion was used for testing. It consists of 37 subjects with 68 beats each, Lead I and estimated Lead I DCT vectors. The parameter for development of the k-means unsupervised classifier was chosen as 37, under the assumption that every Lead I for each subject is different; in which case, every subject will generate a different class. The analysis of the joint distribution between the original subject class and the encoded class showed a mutual information of 4.43 bits, equivalent to 21.5 subject discrimination capacity out of 37; based on the original Lead I DCT. So, this is an upper limit for the performance of the estimator. The same analysis for the *k*-means classifier, $k = 37$, for the estimated Lead-I DCT (based on Lead-1) provides a tighter upper bound of 1.91 bits for the final mutual information between these 2 classifiers, which is finally calculated using Eq. (4) as: 1.6 bits.

4. Discussion and conclusion

The results from this study provide useful information metrics evidence that it is possible to estimate the standard ECG Lead I waveforms, in the P-QRS-T interval, from LUA bipolar leads, with a mean correlation higher than 80%; thus enabling the possibility of monitoring heart rhythm information features from a wearable ECG recording band placed on the LUA, as our prototype development in Fig. 15.

In this study we have only considered single arm leads independently. Based on our observations, it is reasonable to suggest improved methods by combining two or more arm leads simul-

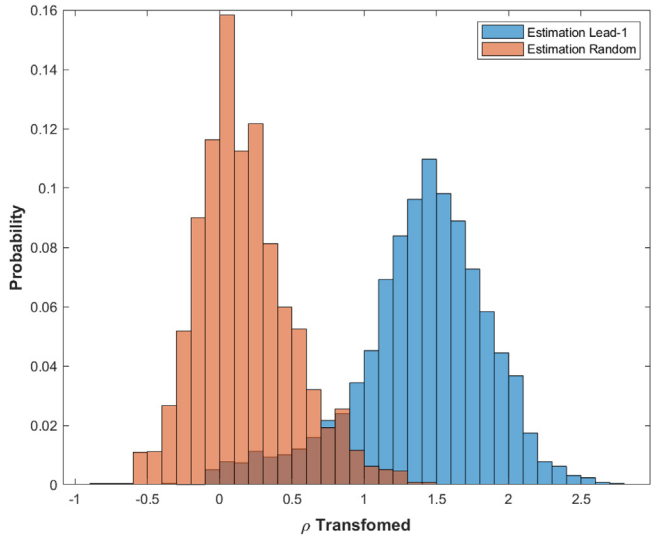

Fig. 13. Transform Histograms of correlation among Lead I and its estimation, when inputs to the ANN are random Lead-1 (brown) and Lead-1 (blue).

Fig. 15. Prototype of LUA wearable band monitoring device (WASTCArD Project), for long-term heart rhythm monitoring.

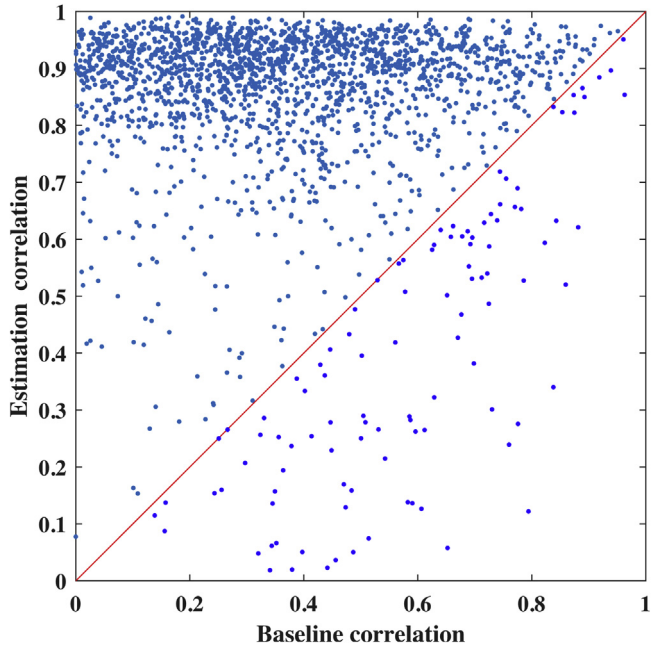

Fig. 14. Plot of estimated correlation and random input Lead-1 estimated correlation. 4.52% (values below red line) of the random input estimation did not improve after the ANN process.

taneously, e.g., Lead-1 and Lead-2; as these two present mutual orthogonal orientation on the LUA.

Even though the DCT is effective for dimensionality reduction, a significant reduction could be obtained from selection of components according to their mean power, instead of using the first 96 coefficients, since the P-QRS-T wave class has characteristic time-frequency features. Further improvements could be investigated by using a compact-support decomposition transform (wavelets) with a possible optimization approach [22].

The ANN has not been optimised; its number of free parameters is too high and sparse. Training with subsets and a hierarchical network, and limiting the connections among the input would significantly reduce its complexity with no significant loss in its performance.

The variability of the P-QRS-T wave in this database is limited as a consequence of the majority of the population having normal electrocardiograms (ECGs). A database with abnormal heart rhythms would be great value [14]. A larger database with standard ECG leads and arm leads currently does not exist. This methodology of estimation used in this study could be used to build such database for abnormal Lead I estimation from abnormal left-arm-lead recordings.

Information theory provides useful and objective measures for evaluating the performance of estimation processes. The analysis also shows, as a side result, that ECG may be used as a biometric characteristic with value comparative to features such as speech.

The main finding in this chest lead I estimation using arm leads, was the capability of the system based on ANN to produce a heartbeat with information about heart rhythm as is shown in Fig. 10 (a), in this figure a smooth P-QRS-T wave form has been well estimated and its correlation with Lead I was 99%.

As it shown in Table 3, correlation criterion acceptance was important to observe the relation between number of subjects used in both, training and testing ANN process in our database. When the ANN is trained with optimum best heartbeats per subject (93% of similarity), there was only one third of the subjects for training (37), and the remaining testing (57), yield to higher correlation among estimated and Lead I in training and lower in testing, which can indicate insufficient subjects in the training set to include most of the P-QRS-T heartbeats morphology in our database and make a good generalization. Further improvement on the generalisation ability may be investigated by adopting a Convolutional Neural Network (CNN) approach and fusing the extracted deep features of a simple CNN and P-QRS-T features [23].

In Table 3 and 4, comparing correlation criterion acceptance of 85%, Lead-1 {0.807 (0.154)} shows better performance among other arm leads, as expected due its higher amplitude and signal to noise ratio [12], comparing to Lead-2 {0.793 (0.217)} and Lead-3 {0.813 (0.171)}.

Some Authors have estimated precordial leads with three bipolar leads [14] and 12-lead ECG using a single beat in a set of three leads [24], thus it will be useful to conduct further studies on ANN training, using some signal quality indexing approach [25] and ECG data fusion from several arm leads.

In conclusion, a clinical multichannel arm-ECG mapping database gathered from 153 subjects, has evidenced through the proposed robust methods in this study, the indication (similarity

correlation coefficient: $\rho > 80\%$) that it is possible to reconstruct the standard ECG Lead I from upper-left-arm bipolar ECG lead recordings, despite significant noise from arm muscle artefact.

Acknowledgments

This research was supported by funds from the European Union (EU): Horizon 2020 Marie Skłodowska-Curie Actions (MSCA) RISE Programme (WASTCArD Project, Grant #645759). Prof Omar Escalona is supported by funds (CACR Project) equally from the Ulster Garden Villages Ltd. and the McGrath Trust, both based in the United Kingdom.

References

[1] E.J. Benjamin, et al., Heart disease and stroke statistics - 2017 update: a report from the american heart association (7/Mar/2017), Circulation 135 (2017), http://dx.doi.org/10.1161/CIR.0000000000000485, 00–00, e390.
[2] P. Zimetbaum, M. Josephson, Evaluation of patients with palpitations, N. Engl. J. Med. 338 (1998) 1369.
[3] G.A. Roth, M.D. Huffman, A.E. Moran, V. Feigin, G.A. Mensah, M. Naghavi, C.I. Murray, Global and regional patterns in cardiovascular mortality from 1990 to 2013, Circulation 132 (2015) 1667–1678, http://dx.doi.org/10.1161/CIRCULATIONAHA.114.008720.
[4] P. Hingorani, D.R. Karnad, P. Rohekar, V. Kerkar, Y. Lokhandwala, S. Kothari, Arrhythmias seen in baseline 24-hour Holter ECG recordings in healthy normal volunteers during Phase 1 clinical trial, J. Clin. Pharmacol. 56 (7) (2016) 885–893, http://dx.doi.org/10.1002/jcph.679.
[5] A.D. Krahn, G.J. Klein, A.C. Skanes, R. Yee, et al., Insertable loop recorder use for detection of intermittent arrhythmias, Pacing Clin. Electrophysiol. 27 (2004) 657–664.
[6] Q. Zhang, D. Zhou, X. Zeng, A novel single-arm-worn 24 h heart disease monitor empowered by machine intelligence, Biomed. Signal Process. Control 42 (2018) 129–133, http://dx.doi.org/10.1016/j.bspc.2018.01.021.
[7] W.D. Lynn, O.J. Escalona, D.J. McEneaney, Arm and wrist surface potential mapping for wearable ECG rhythm recording devices: a pilot clinical study, J. Phys. Conf. Ser. 450 (2013), 012026.
[8] K. Kelly, O.J. Escalona, R.H. Mitchell, The use of adaptive line enhancement for the beat-to-beat detection of late potentials: an evaluation, Innov. et Technol. en Biol. et Med. 13 (1992) 587–600.
[9] O.J. Escalona, et al., A fast and reliable QRS alignment technique for high-frequency analysis of the signal-averaged ECG, Med. Biol. Eng. Comput. 31 (1993) S137–S146.
[10] O.J. Escalona, et al., A robust procedure for P-wave detection and segmentation in high resolution 12-lead ECG, Proceedings of the IEEE-EMBS Annual International Conference vol. 18 (1997) 1365–1366.
[11] W.D. Lynn, O.J. Escalona, P.R. Vizcaya, D.J. McEneaney, Arm-ECG bipolar leads Signal recovery methods for wearable Long-term heart rate and rhythm monitoring, Computing in Cardiology vol. 44 (2017), http://dx.doi.org/10.22489/CinC.2017.072-464.
[12] O. Escalona, W. Lynn, G. Perpiñan, L. McFrederick, D. McEneaney, Data-Driven ECG Denoising Techniques for Characterising Bipolar Lead Sets along the Left Arm in Wearable Long-Term Heart Rhythm Monitoring, Electronics 6 (4) (2017) 84.
[13] A.M. Bianchi, G.D. Pinna, M. Croce, M.T. La Rovere, R. Maestri, E. Locati, S. Cerutti, Estimation of the respiratory activity from orthogonal ECG leads, Computers in Cardiology (2003) 85–88.
[14] J. Lee, M. Kim, J. Kim, Reconstruction of precordial lead electrocardiogram from limb leads using the state-space model, IEEE J. Biomed. Health Inform. 20 (3) (2016) 818–828.
[15] F. Porée, A. Kachenoura, G. Carrault, R. Dal Molin, P. Mabo, A.I. Hernández, Surface electrocardiogram reconstruction from intracardiac electrograms using a dynamic time delay artificial neural network, IEEE Trans. Biomed. Eng. 60 (1) (2013) 106–114.
[16] D. Lynn, Advancement in Wearable, Long-term Heart Rate and Rhythm Monitoring, PhD Thesis, Ulster University, 2017, Mar/.
[17] O. Escalona, L. McFrederick, M. Borge, P. Linares, J. McLaughlin, D. McEneaney, Wrist and Arm body surface cardiac electrogram mappping techniques study for Long-term rhythm monitoring, Computing in Cardiology 44 (2017), http://dx.doi.org/10.22489/CinC.2017.071-458.
[18] T. Cover, J. Thomas, Elements of Information Theory, 2nd ed., Wiley, 2006.
[19] H. Stark, J. Woods, Probability, Statistics, and Random Processes, Pearson Education, 2012.
[20] R.E. Walpole, R.H. Myers, S.L. Myers, K. Ye, Probability and Statistics for Engineers and Scientists, 8th ed., Prentice Hall, 2012 http://fac.ksu.edu.sa/sites/default/files/probability_and_statistics_for_engineers_and_scientisst.pdf.
[21] S. Mann, R. Orglmeister, PCA-based ECG lead reconstruction, Biomed. Tech. Eng. (2013).
[22] Z. Peng, G. Wang, Study on optimal selection of wavelet vanishing moments for ECG denoising, Scientific Reports, Nature 7 (2017) 4564, http://dx.doi.org/10.1038/s41598-017-04837-9.
[23] W. Lu, H. Hou, J. Chu, Feature fusion for imbalanced ECG data analysis, Biomed. Signal Process. Control 41 (2018) 152–160, http://dx.doi.org/10.1016/j.bspc.2017.11.010.
[24] G.R. Tsouri, M.H. Ostertag, Patient-specific 12-lead ECG reconstruction from sparse electrodes using independent component analysis, IEEE J. Biomed. Health Inform. 18 (2) (2014) 476–482.
[25] I. Jekovaa, V. Krastevaa, R. Leberb, R. Schmidb, R. Twerenboldc, T. Reichlinc, C. Müllerc, R. Abächerlic, A real-time quality monitoring system for optimal recording of 12-lead resting ECG, Biomed. Signal Process. Control 34 (2017) 126–133, http://dx.doi.org/10.1016/j.bspc.2017.01.009.